Progress in
Medical Devices

Zentime

REVIEW ARTICLE

Fluorescence-enhanced isothermal amplification for multiplex pathogen detection: Emerging strategies and persistent challenges

Yuanshou Zhu*, Xitian Xu*, Yuxin Chen, Mengyuan Huang, Shoulong Wang, Haoyu Li, Zhigang Zhu

School of Health Science and Engineering, University of Shanghai for Science and Technology, Shanghai 200093, China.
*The authors contribute equally.

Corresponding author: Zhigang Zhu.

Address correspondence to: Zhigang Zhu, School of Health Science and Engineering, University of Shanghai for Science and Technology, No. 516 Jungong Road, Yangpu District, Shanghai 200093, China.
E-mail: zgzhu@usst.edu.cn.

Received March 10, 2026; Accepted March 25, 2026; Published September 10, 2026

DOI: 10.61189/056765fjgmye

Abstract

Multiplex pathogen detection is essential for addressing the increasing complexity of infectious diseases and co-infections, yet conventional polymerase chain reaction-based methods remain hindered by the requirement for sophisticated laboratory infrastructure. Isothermal amplification offers a robust alternative for point-of-care testing, though high-order multiplexing in these systems has historically been limited by signal discrimination challenges. In this review, we synthesize recent breakthroughs in fluorescence-enhanced isothermal amplification, which have transformed multiplex diagnostics through advanced signal encoding and intelligent processing. We illustrate how the convergence of diverse molecular engines, ranging from sequence-specific probes to orthogonal clustered regularly interspaced short palindromic repeats-associated effectors and programmable DNA logic circuits, enables precise, multi-target identification in a single reaction. Beyond the biochemical framework, we further discuss the integration of these molecular strategies with microfluidic platforms, portable optical detection systems, and deep learning-based signal analysis, which collectively facilitate the transition from laboratory prototypes to automated diagnostic platforms. Finally, we examine persistent challenges, including assay crosstalk and amplification bias, and outline future directions toward accessible and scalable multiplex diagnostic systems.

Keywords: Fluorescence strategy, Multiplex pathogen detection, Isothermal amplification, CRISPR diagnostics, Point-of-care testing

Highlights

- Systematic overview of fluorescence-enhanced isothermal amplification strategies for multiplex pathogen detection.
- Comparative analysis of probe-based, clustered regularly interspaced short palindromic repeats-mediated, and strand displacement reaction-programmable multiplex signal encoding mechanisms.
- Emerging integration with microfluidics, portable devices, and deep learning for next-generation point-of-care diagnostics.

1 INTRODUCTION

Global climate change, population migration, and shifts in ecological environments are continuously reshaping pathogen transmission patterns. This dynamic is rendering the epidemic patterns of emerging and re-emerging infectious diseases increasingly complex, with co-infections becoming progressively more common [1-4]. The co-circulation of influenza viruses and severe acute respiratory syndrome coronavirus 2 (SARS-CoV-2), and the synergistic transmission of *Plasmodium*

species and arboviruses in tropical regions, exemplify complex pathogenic mechanisms and pose severe public health challenges [5-7]. Since these infections often present with highly overlapping, non-specific symptoms, differential diagnosis based solely on clinical manifestations is difficult [6]. This can lead to misdiagnosis and the misuse of antimicrobials, exacerbating the risk of antimicrobial resistance [8, 9]. Therefore, achieving efficient and accurate multiplex pathogen detection has become crucial for advancing precision medicine and proactive syndromic surveillance.

Although polymerase chain reaction remains the gold standard for multiplex detection, its dependence on sophisticated thermal cycling equipment and specialized laboratories limits its application in resource-limited settings and point-of-care testing (POCT) scenarios [10, 11]. The ASSURED criteria proposed by the World Health Organization (WHO)—affordable, sensitive, specific, user-friendly, rapid and robust, equipment-free, and deliverable—underscore the importance of accessibility and portability in diagnostic tools [12]. Isothermal nucleic acid amplification techniques, such as loop-mediated isothermal amplification (LAMP) and recombinase polymerase amplification (RPA), achieve efficient nucleic acid amplification at a constant temperature [13-15]. This significantly reduces equipment complexity and enhances the feasibility of on-site testing. However, traditional isothermal methods often rely on turbidity or pH-sensitive colorimetric readouts. These approaches not only suffer from limited sensitivity and quantitative ability but also face inherent difficulties in achieving multiplex detection, severely restricting their application in complex infection scenarios [16-18].

Fluorescence-based signal readout strategies offer a critical technological pathway to overcome these bottlenecks. They not only support real-time quantitative analysis but also enable parallel multi-target detection through spectral discrimination or sequence-specific probes. This significantly enhances the multiplexing capability of isothermal amplification techniques, making them more suitable for complex sample analysis and system integration [19-21]. In recent years, advances in molecular engineering have further propelled the development of fluorescence-based isothermal amplification systems. The clustered regularly interspaced short palindromic repeats (CRISPR) system, with its target-activated trans-cleavage activity, provides a highly specific signal transduction mechanism [22, 23]. Strand displacement reaction (SDR) and other nucleic acid nanotechnology tools are being used to construct programmable signal logic and cascaded amplification networks, further enhancing the signal-to-noise ratio and multi-target decoding capability of detection systems [24]. At the systems level, the integration of microfluidic chips, portable optical readers, and intelligent signal analysis algorithms is continuously propelling molecular diagnostic platforms toward higher integration, automation, and on-site applicability [25, 26].

Despite rapid technological progress, several core challenges remain in developing stable, reliable, and scalable multiplex fluorescence-based isothermal detection systems. These include the rapid increase in system complexity due to cross-reactivity between primers and probes; spectral crosstalk between multiple fluorescent signals limiting detection throughput; and differences in amplification kinetics among multiple targets that affect quantitative accuracy [15, 27, 28]. In light of these challenges, this review aims to systematically synthesize the latest advances in fluorescence-based isothermal amplification strategies for multiplex pathogen detection. We first dissect the core molecular toolbox used to construct these detection systems, elucidating the intrinsic characteristics and working principles of LAMP, RPA, CRISPR, and SDR. Next, we discuss three mainstream fluorescence multiplex detection strategies: probe design based on spectral discrimination, multi-signal transduction based on orthogonal CRISPR enzymes, and programmable logic and cascaded amplification based on SDR. Finally, we review the development trends in microfluidic systems, portable detection devices, and intelligent signal analysis technologies. By constructing a holistic technological framework that spans from fundamental molecular principles to system-level engineering implementation, this review aims to provide theoretical insights and design ideas for the development of next-generation molecular diagnostic platforms characterized by high sensitivity, high specificity, and on-site deployability for multiplex detection.

2 CORE MOLECULAR TOOLBOX

Constructing high-performance multiplex nucleic acid detection systems first requires a deep understanding of the molecular tools that form their technological core. Based on their functional roles in the detection workflow, these tools can be categorized into two main groups: nucleic acid amplification engines for target enrichment and signal transduction modules for specific recognition and signal conversion. This section systematically dissects the molecular mechanisms and intrinsic characteristics of four core technologies—LAMP, RPA, CRISPR systems, and SDR—laying the theoretical foundation for subsequent discussions on their integrated application in multiplex detection (**Figure 1**).

2.1 LAMP: Efficient amplification and structured products

LAMP, first reported by Notomi et al. in 2000, has become one of the most widely adopted isothermal amplification techniques [29]. This method primarily relies on *Bacillus stearothermophilus* DNA polymerase, which possesses high strand displacement activity, together with a set of 4–6 primers that recognize 6–8 distinct regions within the target sequence, enabling efficient amplification under isothermal conditions (60–65 °C) [15]. The amplification mechanism involves two phases: an

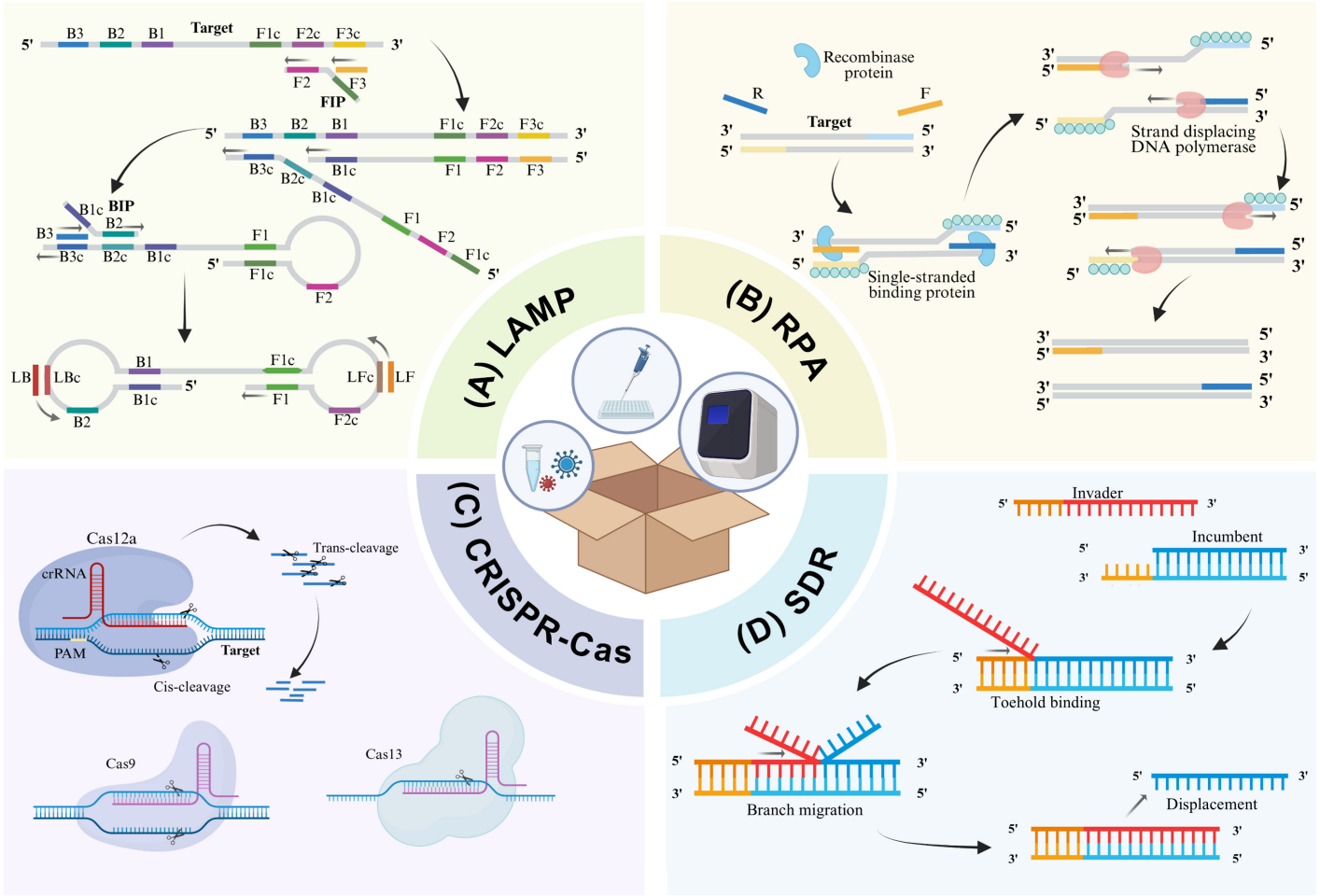

Figure 1. Schematic illustration of the core molecular toolbox. (A) Principle of the LAMP reaction; (B) Principle of the RPA reaction; (C) Mechanisms of CRISPR cis-cleavage and trans-cleavage; (D) Mechanism of SDR. LAMP, loop-mediated isothermal amplification; RPA, recombinase polymerase amplification; CRISPR, clustered regularly interspaced short palindromic repeats; Cas, CRISPR-associated; Cas12a, CRISPR-associated protein 12a; Cas9, CRISPR-associated protein 9; Cas13, CRISPR-associated protein 13; SDR, strand displacement reaction; FIP, forward inner primer; BIP, backward inner primer; F, forward primer; R, reverse primer; LF, loop forward primer; LB, loop backward primer; crRNA, CRISPR RNA; PAM, protospacer-adjacent motif. F1, F2, F3, B1, B2, and B3 indicate target sequence regions in LAMP primer design; the suffix "c" indicates the complementary sequence.

initial structure-formation phase and a subsequent cyclic amplification phase. As illustrated in **Figure 1A**, during the initiation phase, the inner primers, forward inner primer (FIP) and backward inner primer, first hybridize to the target sequence, initiating strand displacement synthesis. Subsequently, the outer primers, forward outer primer and backward outer primer further displace the newly synthesized strand and release single-stranded DNA (ssDNA), forming a loop structure that serves as a template for further amplification. In the cyclic amplification phase, these loop structures are continuously recognized and extended by primers, ultimately generating characteristic "cauliflower-like" amplification products composed of stem-loop structures of varying sizes [16].

This unique amplification mechanism endows LAMP with three intrinsic properties critical for downstream detection. First, its exceptionally high amplification efficiency provides abundant molecular substrates for fluorescence signal detection, forming the basis for LAMP's high sensitivity [15, 30]. Second, the complex 'cauliflower-like' structures offer numerous recognition sites for the hybridization of sequence-specific fluorescent probes. Third, its excellent matrix tolerance allows LAMP to maintain amplification activity in crude samples containing common inhibitors such as hemoglobin, heparin, and ethanol, often enabling detection directly from heat-lysed samples without the need for extensive nucleic acid purification [31, 32]. It should be noted, however, that while LAMP's high specificity relies on the cooperative recognition of 6–8 target regions by multiple primers, this mechanism can lead to primer-primer interactions and an increased risk of non-specific amplification in multiplex settings, which severely complicates probe design and cross-reactivity mitigation [33].

2.2 RPA: Low-temperature reaction and rapid initiation

RPA, first reported by Piepenburg et al. in 2006, is an isothermal nucleic acid amplification method that has gained considerable attention in recent years [34]. RPA mediates nucleic acid amplification through the coordinated action of recombinase, ssDNA-binding proteins, and a strand-displacing DNA polymerase, mimicking the process of *in vivo* DNA recombination [14]. At a constant temperature (37–42 °C), recombinase first forms complexes with primers, scanning double-stranded DNA templates for complementary sequences. Upon successful recognition, the recombinase facilitates primer invasion into the double-stranded template. ssDNA-binding proteins subsequently stabilize the displaced ssDNA region, and the polymerase extends the primer to initiate exponential amplification (**Figure 1B**). The entire process is typically completed within 20–40 min [35].

RPA's most significant intrinsic characteristics are its low-temperature reaction conditions and low dependence on sample purity. The optimal reaction temperatures for most CRISPR effector proteins, such as CRISPR-associated protein 12a (Cas12a) and CRISPR-associated protein 13a (Cas13a), also cluster in the 37–42 °C range [27, 28]. This temperature compatibility provides ideal conditions for one-pot amplification-detection systems, offering a significant advantage over LAMP systems (60–65 °C), which require thermostable CRISPR-associated (Cas) protein variants or complex physical segregation strategies [36]. Furthermore, because the recombinase-mediated strand invasion process is relatively insensitive to common sample inhibitors (e.g., heme, humic acid), RPA can often be performed directly on crude lysates without requiring highly purified nucleic acid templates, reducing the threshold for sample processing [34, 37]. However, RPA systems also present specific technical caveats: the reaction typically requires the addition of high-molecular-weight polymers, such as polyethylene glycol, as molecular crowding agents to maintain recombinase activity, which can increase system viscosity [38]. Concurrently, the continuously active recombinase may interfere with bound fluorescent probes, potentially affecting the stability of real-time signal readouts [14, 35]. This interference is magnified in multiplex detection systems, imposing higher demands on probe design and reaction kinetics.

2.3 CRISPR systems: Specific recognition and signal transduction

The CRISPR system is an adaptive immune defense mechanism found in bacteria and archaea that functions to recognize and cleave foreign nucleic acids [39]. Based on the composition and function of its effector proteins, it can be classified into two classes, six types, and several subtypes [40, 41]. While initially garnering widespread attention for its revolutionary applications in genome editing, specific effector families such as CRISPR-associated protein 12 and CRISPR-associated protein 13 possess unique nucleic acid targeting and cleavage properties that make them ideal tools for nucleic acid detection [23, 27, 42].

The core function of CRISPR systems in detection applications stems from their target-activated trans-cleavage activity, which relies on specific recognition coupled with non-specific cleavage [23, 43]. The Cas12a/CRISPR RNA (crRNA) complex achieves recognition through complementary pairing between the crRNA and the target DNA, simultaneously requiring the presence of a conserved protospacer-adjacent motif (PAM; typically 5'-TTTN-3') adjacent to the target sequence [23]. The Cas13a/crRNA complex recognizes target RNA and requires a protospacer flanking sequence (PFS) downstream of the target, although the stringency of the PFS varies among different Cas13a orthologs [22, 44]. This dual-recognition mechanism of crRNA complementarity and PAM/PFS requirement grants CRISPR systems high specificity, providing a molecular basis for distinguishing highly homologous sequences within complex samples. Specific recognition triggers a conformational change in the Cas protein, exposing its catalytic domain (e.g., the RuvC domain of Cas12a and the higher eukaryotes and prokaryotes nucleotide-binding domains of Cas13a) and activating sequence-independent trans-cleavage activity (**Figure 1C**) [23, 45]. Upon target DNA recognition, Cas12a acquires the ability to non-specifically cleave any ssDNA in its vicinity. Similarly, target RNA recognition activates Cas13a's ability to non-specifically cleave any single-stranded RNA (ssRNA) [22, 23].

This mechanism enables an elegant signal transduction strategy. Specifically, an ssDNA or ssRNA reporter molecule is labeled at opposite ends with a fluorophore and a quencher, maintaining the fluorescence in an initially quenched state. Upon recognition of the target, the activated Cas protein cleaves the reporter, separating the fluorophore from the quencher and releasing a detectable fluorescent signal [46]. This direct coupling between target recognition and signal conversion positions the CRISPR system not merely as a highly specific recognition element but also as an efficient signal transduction module.

2.4 SDR: Programmable signal amplification and logic control

SDR is a class of molecular reaction mechanisms governed by the thermodynamics and kinetics of complementary nucleic acid hybridization [47]. Its core feature lies in the structural rearrangement and information transfer among multiple nucleic acid strands driven by competitive pairing, a principle which relies on the predictable thermodynamics of Watson-Crick base pairing [48].

The basic mechanism of SDR involves an 'invader' strand displacing an 'incumbent' strand from a duplex, driven by the

reduction in the system's net Gibbs free energy (ΔG). When the invader strand is fully complementary to an exposed single-stranded region (the "toehold") on the duplex, it can initiate branch migration and ultimately completely displace the incumbent strand (**Figure 1D**). This process allows for the construction of complex, enzyme-free reaction networks, enabling molecular computation, signal amplification, and precise regulation of downstream effectors [49, 50].

Hybridization chain reaction is a representative example of SDR used for enzyme-free signal amplification [51]. This technique utilizes two kinetically trapped hairpin structures that store chemical potential energy—their stems are sealed by short complementary regions, preventing spontaneous opening. When a target trigger strand is present, it binds to the toehold region of the first hairpin and unfolds it. The newly exposed single-stranded region subsequently opens the second hairpin. This process propagates in a cascade manner, ultimately forming a long nicked double-stranded polymer. Hybridization chain reaction operates under isothermal conditions, often even at room temperature, converting a single target recognition event into a significantly amplified fluorescent signal, thus making it a commonly used downstream signal amplification module in isothermal amplification systems [52, 53].

Toehold-mediated strand displacement (TMSD) focuses more on the precise regulation of reaction kinetics. The introduction of a short single-stranded overhang (the 'toehold') at the terminus of a duplex complex, it provides a controllable nucleation site for the invader strand, transforming the strand displacement process from a simple hybridization reaction into a programmable kinetic switch. Studies have demonstrated that by modulating toehold length (typically 5–7 nt) and sequence composition, the strand displacement rate can be finely tuned over several orders of magnitude, enabling signal regulation across different timescales [50]. Computational nucleic acid design tools (e.g., Nucleic Acid Package, oxDNA) are routinely employed in this process to predict secondary structures and thermodynamic profiles [54, 55]. Furthermore, the modular design of SDR allows for the construction of complex molecular logic circuits, such as AND gates, OR gates, and cascaded amplification [56]. This enables SDR to function as intelligent middleware, performing logical operations and noise reduction on raw signals generated by upstream amplification, thereby achieving advanced integration of multiplex signals without the need for complex electronic instrumentation.

In summary, the landscape of isothermal multiplex detection is defined by a strategic trade-off between amplification efficiency and target specificity. Nucleic acid amplification engines, including LAMP and RPA, excel at rapid substrate generation in crude matrices at low temperatures, yet they are inherently prone to primer-induced crosstalk in multiplexed formats. Signal transduction modules, such as CRISPR-Cas systems and SDR-based circuits, offer unparalleled molecular precision, effectively transforming biological recognition into programmable, noise-free signal outputs. These modules are not devoid of limitations; CRISPR systems often necessitate complex orthogonal enzyme combinations, while SDR-based logic circuits require stringent sequence design that may be vulnerable to interference in complex biological samples. Given that no single technology can simultaneously fulfill all the rigorous demands of an ideal multiplex assay, the most promising trajectory for the field lies in decoupling the amplification phase from the recognition/signaling phase. By synergizing the high-efficiency amplification of LAMP/RPA with the exquisite specificity and logic-gated control of CRISPR and SDR, researchers can construct robust, interference-free diagnostic networks. The subsequent discussions will focus on how these tools are ingeniously hybridized to achieve scalable multiplexing and integrated into automated, intelligent POCT platforms.

3 FLUORESCENCE-BASED MULTIPLEX DETECTION STRATEGIES IN ISOTHERMAL AMPLIFICATION

In isothermal amplification, the core challenge in multiplex detection is the simultaneous identification of multiple targets within a single reaction while generating distinguishable signal outputs. Building upon the molecular toolbox introduced in the previous section, diverse research efforts have progressively developed a range of multiplex detection strategies. These strategies exhibit significant differences in signal encoding methods, system complexity, and scalability. From a technological perspective, current fluorescence-based multiplex isothermal amplification strategies can be broadly categorized into three classes. The first relies on differences in fluorescence spectra for signal discrimination, employing multiple fluorescent probes within a single tube to report different targets. The second leverages the enzymatic orthogonality among different CRISPR systems to construct parallel signal transduction pathways, achieving target differentiation at the molecular level. The third utilizes the programmable properties of SDRs, enabling molecular logic operations and cascaded signal amplification for more complex signal encoding and decoding.

3.1 Fluorescent probes for multiplex detection

The most direct approach to multiplex detection involves designing multiple reporter probes with distinct fluorescence emission wavelengths, allowing different targets within a single reaction system to generate distinguishable fluorescent signals. This strategy primarily relies on fluorescence spectral discrimination for target differentiation, making it technically one of the simplest and earliest multiplex detection strategies to be developed [57]. Based on their signal-generation mechanisms, existing strategies can be classified into three main types: hydrolysis-dependent, conformation-dependent, and cleavage-dependent probes [20].

3.1.1 Hydrolysis-dependent probes

The core mechanism of hydrolysis-dependent probes is analogous to that of the classic TaqMan probes used in polymerase chain reaction, relying on the irreversible degradation of the probe by an exonuclease upon hybridization with the target, thereby releasing a fluorescent signal [21]. In isothermal amplification systems, a representative implementation of this strategy is the Exo probe used in RPA [34]. Exo probes typically contain an internal abasic site mimic (tetrahydrofuran) that is flanked by a fluorophore and a quencher, with the 3' end usually blocked to prevent primer extension. When the probe specifically binds to the single-stranded target generated during amplification, the nuclease Exonuclease III present in the RPA system recognizes the tetrahydrofuran site within the resulting duplex and cleaves the probe. This hydrolysis permanently separates the fluorophore from the quencher, leading to an irreversible accumulation of fluorescence.

The use of target-specific Exo probes labeled with spectrally distinct fluorophores enables multiplex pathogen detection. In the seminal study on RPA, Piepenburg et al. first introduced Exo probes into an isothermal amplification system [34]. By employing a combination of universal and specific primers, alongside dual-labeled fluorescent probes and an internal amplification control, they successfully demonstrated single-tube multiplex detection of three methicillin-resistant *Staphylococcus aureus* subtypes, thereby validating the potential of RPA for pathogen typing.

3.1.2 Conformation-dependent probes

Conformation-dependent probes rely on target-induced changes in secondary structure to switch fluorescence signals on or off. Molecular beacons (MBs) represent a typical example of this class of probes. Their stem-loop structure positions the fluorophore and quencher in close proximity, while the loop sequence is complementary to the target. Talap et al. utilized MBs to construct a dual-fluorescence reverse transcription LAMP system, enabling simultaneous detection of the SARS-CoV-2 nucleocapsid gene and open reading frame 1ab in a single tube [58].

Detection of amplification by release of quenching was first proposed by Tanner et al. and generates real-time fluorescent signals by using separate probe molecules during amplification [18]. The core design involves labeling the 5' end of the FIP primer with a quencher, while a short displacement probe (Fd) complementary to the F1c region is labeled with a fluorophore at its 3' end. Upon annealing, the FIP and Fd form a duplex where the fluorophore is quenched. During LAMP amplification, strand extension from the opposite primer leads to displacement and release of the Fd probe. As a result, the fluorophore becomes spatially separated from the quencher, generating a fluorescence signal. This mechanism enables multiplex detection of up to four targets in a single tube, by assigning distinct fluorophores, such as 6-carboxyfluorescein (FAM), hexachlorofluorescein (HEX), carboxy-X-rhodamine (ROX), and cyanine 5 (Cy5), to different targets and monitoring the signals in separate fluorescence channels in real time.

The quenching of unincorporated amplification signal reporters (QUASR) technology demonstrates an alternative based on temperature-dependent conformational modulation. Ball et al. labeled the 5' end of either the backward inner primer or FIP primer with a fluorophore, simultaneously introducing a short (7–13 nucleotides) quencher probe complementary to the 5' end of the labeled primer, which is modified with a quencher at its 3' end [57]. The melting temperature of the quencher probe is designed to be significantly lower than the reaction temperature (<55 °C). During the high-temperature amplification phase, the quencher probe dissociates without interfering with primer extension. Upon cooling after the reaction, unincorporated free primers bind to the quencher probe, causing fluorescence quenching, while primers incorporated into the double-stranded amplification product retain high fluorescence. This 'end-point quenching' mechanism allows QUASR to achieve signal-to-noise ratios up to 8:1 and has been successfully applied to single-tube duplex detection of West Nile virus and chikungunya virus (CHIKV). Priye et al. further integrated QUASR with a smartphone platform to develop a portable diagnostic system for the simultaneous detection of Zika virus, CHIKV, and dengue virus, providing a complete solution for on-site applications in resource-limited settings [37]. Yang et al. introduced QUASR into a hydrogel-based digital LAMP platform [59]. By forming a polyethylene glycol-crosslinked hydrogel network, amplification products were immobilized *in situ* as stable fluorescent microgels. By labeling FIP primers targeting different pathogens with spectrally distinct fluorophores, the resulting spot color served as an indicator of the bacterial type, while the spot count directly correlated with bacterial concentration, thereby achieving duplex absolute quantification of methicillin-resistant *Staphylococcus aureus* and carbapenem-resistant *Escherichia coli*.

3.1.3 Cleavage-dependent probes

Cleavage-dependent probes generate fluorescent signals through a cascade of recognition, cleavage, and release events. This mechanism is typically facilitated by the incorporation of enzymes with specific cleavage activities. The advantage of this strategy lies in leveraging the strict substrate specificity of these enzymes, which can significantly reduce the risk of false positives caused by non-specific amplification.

The multiple endonuclease restriction real-time LAMP technique, developed by Wang et al., enables rapid differentiation of *Listeria* species by incorporating recognition sites for a restriction endonuclease, such as Nb.BsrDI, into the primers [60]. Upon successful primer extension and double-stranded

target formation, the endonuclease cleaves the fluorophore-quencher linkage within the primer, thereby releasing the fluorescent signal. This method exploits the strict substrate specificity of the enzyme, substantially reducing false-positive signals arising from non-specific amplification. Higgins et al. developed *Thermus thermophilus* endonuclease cleavage LAMP, which utilizes the cleavage activity of *Thermus thermophilus* endonuclease IV at abasic sites [61]. In a quadruplex detection system, this technique enables the real-time monitoring of pathogens, such as *Streptococcus pneumoniae* and *Neisseria meningitidis*, demonstrating sensitivity comparable to that of quantitative polymerase chain reaction (qPCR) while offering a significantly simplified workflow.

The proofreading enzyme-mediated probe cleavage (Proofman) technique offers an alternative strategy by exploiting the intrinsic 3'-to-5' exonuclease proofreading activity of high-fidelity DNA polymerases. Ding et al. designed fluorescent probes with a deliberate mismatch at the 3' end [62]. When the probe hybridizes correctly with the target sequence, *Pyrococcus furiosus* polymerase removes the fluorophore-labeled mismatched nucleotide at the 3' terminus, thereby generating a fluorescence signal. This mechanism not only enables multiplex detection but also improves amplification efficiency, as the cleaved probe can function as a primer for subsequent extension. Building on this principle, Dong et al. developed a high-fidelity DNA polymerase-mediated probe (HFman), which utilizes Q5 polymerase to achieve single-tube triplex detection of SARS-CoV-2, influenza virus, and an internal control gene [63]. Furthermore, this method demonstrates significant robustness in the direct detection of clinical nasopharyngeal swab samples, eliminating the need for nucleic acid extraction.

3.2 CRISPR system for multiplex detection

As discussed previously, Cas12a cleaves ssDNA, Cas13a cleaves ssRNA, and different Cas13a orthologs exhibit distinct cleavage preferences depending on the base composition of ssRNA. These substrate orthogonal substrate specificities provide a natural enzymatic dimension for achieving single-tube multiplex detection [27, 64]. The core principle of orthogonal Cas effector combination strategies involves deploying multiple orthogonal effectors within a single reaction system, each designed to recognize a specific target and generate an output signal via spectrally distinguishable reporter molecules [65].

Gootenberg et al. pioneered the use of CRISPR enzymatic orthogonality for multiplexing within the specific high-sensitivity enzymatic reporter unlocking version 2 platform [27]. The research team conducted a systematic screen of the substrate cleavage preferences of 3 Cas13a and 14 CRISPR-associated protein 13b (Cas13b) orthologs, identifying unique dinucleotide sequence preferences for each enzyme. Notably, *Leptotrichia wadei* Cas13a preferentially cleaves AU sequences, *Capnocytophaga canimorsus* Cas13b targets UC sequences, and *Prevotella* sp. MA2016 Cas13b exhibits a bias toward GA sequences. Building on these findings, they combined *Leptotrichia wadei* Cas13a (AU reporter, Cy5 channel), *Prevotella* sp. MA2016 Cas13b (GA reporter, FAM channel), *Capnocytophaga canimorsus* Cas13b (UC reporter, Texas Red channel), and *Acidaminococcus* sp. Cas12a (ssDNA reporter, HEX channel) in a single reaction system. This assembly achieved the simultaneous detection of four distinct targets, including Zika virus, dengue virus, and synthetic RNA/DNA templates. To further enhance detection sensitivity, the specific high-sensitivity enzymatic reporter unlocking version 2 platform also incorporated a CRISPR-associated Rossmann fold protein 6 (Csm6) signal amplification system. Following CRISPR-associated protein 13-mediated cleavage of RNA reporters, the resulting fragments carry 2',3'-cyclic phosphate termini, which can act as natural activators of Csm6. Once activated, Csm6 subsequently cleaves its own specific reporter molecules, generating a signal cascade that increases the overall signal intensity by approximately 3.5-fold.

The CRISPR multiplexed diagnostic assay platform, reported by Ghouneimy et al., advances the orthogonal Cas effector strategy for point-of-care applications [36]. This study employed three thermostable CRISPR effectors—*Alicyclobacillus acidiphilus* Cas12b, *Thermoclostridium caenicola* Cas13a, and *Herbinix hemicellulosilytica* Cas13a—integrated with LAMP to enable the single-tube, one-step simultaneous detection of high-risk human papillomavirus (HPV) type 16, HPV type 18, and the human internal control gene, ribonuclease P. The innovation of this strategy lies in leveraging the synergistic temperature compatibility and substrate orthogonality of these enzymes. All enzymes function at 56 °C, fully compatible with the LAMP amplification temperature. HPV type 16 was detected by *Alicyclobacillus acidiphilus* Cas12b using a ROX-labeled ssDNA reporter, HPV type 18 by *Herbinix hemicellulosilytica* Cas13a using a FAM-labeled polyuridine RNA reporter, and ribonuclease P by *Thermoclostridium caenicola* Cas13a using a HEX-labeled RNA mix reporter. Rigorous cross-validation confirmed the system's high orthogonality and signal independence, with a limit of detection (LOD) of 10 copies/μL and full concordance observed in clinical triplex testing. While orthogonal Cas combinations effectively utilize the enzymatic dimension, mitigating potential interference among multiple guide RNA (gRNA)-Cas complexes and ensuring equitable target competition within a single reaction vessel remains a critical challenge.

Le et al. advanced the orthogonal Cas effector strategy by developing a duplex RPA-CRISPR/Cas12a/13a assay for foodborne virus detection [28]. Targeting genogroup I norovirus and group A rotavirus, the method exploits distinct Cas-mediated recognition mechanisms. To accommodate the high sequence variability of the genogroup I norovirus genome, Cas12a was employed to detect its DNA amplification product via a ROX-labeled ssDNA reporter. Conversely, for the highly

conserved viral protein 6 gene of group A rotavirus, the RPA primers were appended with a T7 promoter; subsequent T7-mediated transcription generated RNA targets for Cas13a-based detection using a FAM-labeled ssRNA reporter. In simultaneous single-tube assays, the presence of both viruses triggers dual-channel signals (ROX and FAM), which can be visualized as a yellow fluorescent color under blue light. This method achieved an LOD of 10^2 copies/μL with no cross-reactivity observed among common foodborne pathogens. Furthermore, the system's practical utility was validated in spiked strawberry and lettuce matrices.

3.3 SDR for multiplex detection

SDR is characterized by toehold-mediated kinetic control, the capacity to construct Boolean logic gates, and the potential for enzyme-free cascading amplification. Integrating the specific recognition capability of CRISPR systems with the programmable signal conversion mechanisms of SDR has emerged as a significant approach for achieving high-plex, high-specificity multiplex detection. A common feature of these strategies is the exploitation of the cis-cleavage activity of CRISPR effectors to induce defined structural changes, which then trigger downstream SDR networks. Distinct fluorescent outputs are subsequently used to differentiate multiple targets.

The CRISPR-associated protein 9 (Cas9) R-loop usage for molecular beacon opening (COLUMBO) platform, developed by Marquez-Costa et al., exploits the inherent absence of trans-cleavage activity in *Streptococcus pyogenes* Cas9 [56]. It couples Cas9 R-loop formation with MB opening, enabling CRISPR-mediated strand displacement for multiplex detection. In this assay, target recognition by the single-guide RNA-Cas9 complex displaces the non-target strand, which subsequently hybridizes with a target-specific MB, triggering its opening and fluorescence emission. Using target-specific single-guide RNAs and spectrally distinct beacons, COLUMBO allows single-tube, parallel detection of multiple viral targets, including SARS-CoV-2. Beyond simple detection, COLUMBO integrates biological recognition with DNA strand displacement circuits to enable programmable molecular information processing. By configuring tripartite ssDNA complexes, COLUMBO implements Boolean logic: OR gates respond to either target via single-input strand displacement, whereas AND gates require concurrent binding of two displaced strands to cooperatively release a central fluorophore-labeled strand. This logic-gated design enhances diagnostic specificity and facilitates sophisticated molecular diagnostics, such as conditional signaling during co-infections.

The CRISPR-TMSD platform, developed by Fu et al., combines the cis-cleavage activity of Cas12a with TMSD to achieve multiplex nucleic acid detection using a single Cas protein [66]. The core mechanism involves Cas12a, guided by a crRNA, specifically cleaving the target DNA to generate an 8-nucleotide sticky end, which serves as the trigger strand for the TMSD reaction. Unlike traditional trans-cleavage-based CRISPR assays, this platform operates via an 'inversely coupled' logic: the presence of the target promotes the hybridization of the trigger strand to an inhibitor strand, thereby arresting the SDR and suppressing fluorescence. In the absence of the target, strand displacement proceeds unimpeded, leading to fluorophore-quencher separation and signal emission. This design effectively transforms target recognition into a logic-gated switch. By customizing crRNAs and corresponding overhangs coupled with unique toehold sequences and fluorescent reporters, the platform enables logical discrimination of multiple targets within a single reaction vessel. To optimize signal resolution, the team incorporated locked nucleic acid modifications into the toehold regions, using the oxDNA simulation platform to precisely tune the toehold length and locked nucleic acid density, thereby ensuring high orthogonality across detection channels. This platform has been successfully applied to the discrimination of three epidermal growth factor receptor gene mutations and three SARS-CoV-2 variants.

The toehold activator strategy illustrates how SDR can leverage thermodynamic control to enhance the single-base resolution of CRISPR detection [67]. Traditional Cas12a detection relies on PAM sequence recognition and exhibits a significant tolerance for single-base mismatches in regions distal to the PAM site. By contrast, the toehold activator strategy bypasses strict PAM requirements through a thermodynamically gated activation mechanism, wherein Cas12a activation is strictly governed by the thermodynamic stability of an SDR. In this design, a double-stranded DNA activator contains a single-stranded toehold region, which the crRNA must fully engage via strand displacement to activate Cas12a. Although this technique is currently primarily limited to singleplex applications, its core mechanism offers a viable pathway for single-tube multiplex detection by integrating multicolor fluorescent reporter systems and multiple orthogonal toehold activators [68].

SDR circuits enhance multiplex detection capacity through several key mechanisms. The programmability of TMSD enables orthogonal reaction pathways that operate in parallel within a single vessel, effectively creating independent molecular channels for signal transduction. SDR circuits can be designed as molecular logic gates that integrate signals from multiple targets and generate distinct outputs only upon specific target combinations, facilitating conditional detection of co-infections. SDR-based amplification strategies further enable enzyme-free signal cascades that amplify fluorescence without introducing enzymatic background noise, thereby preserving the fidelity of multiplexed readouts. These features position SDR as a versatile middleware layer that links target recognition facilitated by CRISPR or upstream amplification to fluorescence signal generation, enabling multiplexing capabilities beyond the constraints of spectral discrimination alone.

Based on these three signal-encoding strategies, **Table 1** summarizes representative studies, including their underlying mechanisms, technical characteristics, and performance metrics, thereby facilitating direct comparison of their applicability and scalability in multiplex pathogen detection.

4 PORTABLE READOUT AND INTELLIGENT ANALYSIS

Although innovations in the molecular toolbox and detection strategies have provided a robust biochemical foundation for multiplex pathogen detection, translating these laboratory-based techniques into POCT products that meet the ASSURED criteria remains a significant engineering challenge. This section delineates the systemic integration required to bridge this gap, discussing how portable optical readers facilitate efficient signal acquisition, how microfluidic architectures automate complex fluid handling, and how artificial intelligence (AI) algorithms empower the intelligent analysis of high-dimensional data. Collectively, these advancements are driving the transition of molecular diagnostics toward on-site, intelligent, and autonomous platforms.

4.1 Portable optical readers: Miniaturization and low power consumption

4.1.1 Smartphone-integrated platforms

Smartphones, owing to their ubiquity, powerful computational capabilities, and high-quality imaging sensors, have become the preferred platform for developing portable optical readers. The 'LAMPbox' hardware architecture developed by Priye et al. comprises a 5 V Universal Serial Bus-powered heating module (consuming only 85 mW; stable at 67±1 °C), an optical module integrated with a 3 W red-green-blue (RGB) light-emitting diode (LED) and multi-bandpass filters, and an Arduino Uno-based control module with Bluetooth connectivity [37]. The smartphone app 'LAMPoGo' facilitates wireless control of thermal and optical parameters, enabling real-time temperature monitoring and fluorescence imaging. To enhance detection accuracy, the team implemented Commission Internationale de l'Éclairage xyY color space conversion, transforming raw RGB images into chromaticity coordinates (x, y) and luminance values (Y). In this approach, distinct fluorescent signals are mapped onto predefined 'islands' within the chromaticity space, enabling intuitive multiplex differentiation. By decoupling luminance from chromatic information, this algorithm achieves a 3.2–6.4-fold improvement in signal-to-noise ratio compared with traditional RGB intensity analysis (**Figure 2A**).

Yu et al. integrated a smartphone with Cas12a detection and a microfluidic chip to develop a portable platform capable of digital and multiplex nucleic acid detection [25]. As shown in **Figure 2B**, the three-dimensional-printed smartphone attachment contains a 465 nm laser diode, a 525/15 nm bandpass filter, and a 16 mm external lens, and is powered by three AAA batteries. In a complementary approach, Ball et al. used high-power LEDs (10 W, blue 465 nm, green 523 nm, red 623 nm) as excitation sources, combined with corresponding bandpass filters [57]. An LED light source was used for excitation, and a single-layer plastic filter film served as the emission filter, enabling both naked-eye visualization and smartphone imaging. In duplex detection validation, when excited with a green LED and observed through a 550 nm long-pass filter, only West Nile virus-positive samples appeared red. When excited with a blue LED and observed through a green filter, only CHIKV-positive samples appeared green. Samples positive for both targets produced a composite yellow signal. This design demonstrates that multiplex fluorescence detection can be achieved using a smartphone coupled with simple optical accessories.

4.1.2 Handheld dedicated devices

Beyond smartphone-based attachments, researchers have developed stand-alone handheld diagnostic devices integrating heating, optical detection, and wireless communication capabilities, which provide enhanced operational autonomy and field robustness.

The WeD-1 handheld isothermal fluorescence detection device, developed by Pang et al., was specifically designed for on-site detection of aquatic pathogens [46]. The device weighs only 280 g and is compact enough to be carried in a backpack. It features a three-dimensional-printed casing and a computer numerical control-machined aluminum heating block equipped with a built-in proportional-integral-derivative temperature control algorithm to ensure precise temperature regulation. The optical module consists of a 480 nm excitation LED and a 500–670 nm bandpass filter. A viewing window on the top of the device allows direct visual observation of fluorescence color changes. The device connects to a smartphone application via Bluetooth, enabling real-time temperature program configuration, reaction temperature monitoring, and fluorescence signal observation (**Figure 2C**). Combined with an enhanced one-tube LAMP–*Pyrococcus furiosus* Argonaute detection method, this platform achieved duplex visual detection of largemouth bass iridovirus and *Enterocytozoon hepatopenaei* in shrimp.

The point-of-care kit for the entire test platform, developed by Xu et al., represents another ultra-portable, workflow-integrated design concept [69]. As depicted in **Figure 2D**, the platform weighs less than 100 g and measures under 25 cm, allowing it to be stored within a B5-sized envelope. The architecture consists of an integrated chip (i-chip) for DNA extraction, purification, and signal amplification, paired with a foldable cardboard housing (f-box) that serves as the smartphone interface. This housing integrates an LED source and a smartphone cradle, leveraging the device's native capabilities for thermal regulation, optical detection, and data readout. The platform's clini-

Table 1. Summary of representative fluorescence-enhanced isothermal amplification strategies for multiplex pathogen detection

Technology category	Technique name	Signal generation mechanism	Enzyme/protein	Detection target(s)	Number of targets	Temperature	LOD	Ref.
Hydrolysis-dependent probes	RPA	RPA+Exo probe	Exonuclease III	MRSA I, MRSA II, and MRSA III	3	37 °C	10 copies/reaction	[34]
Conformation-dependent probes	RT-LAMP-MB	RT-LAMP+MB probe	NA	SARS-CoV-2 ORF1ab, N	2	54 °C	ORF1ab: 20 copies/μL; N: 2 copies/μL	[58]
	DARQ	RT-LAMP+DARQ probe	NA	*E. coli* dnaE, λ phage DNA, human CFTR, human BRCA1, *C. elegans* lec-10	4	65 °C	<100 copies/reaction	[18]
	QUASR	RT-LAMP+QUASR probe	NA	WNV, CHIKV	2	63–65 °C	2–100 PFU equivalents/reaction	[57]
	QUASR	RT-LAMP+QUASR probe	NA	ZIKV, CHIKV, DENV-1	3	67 °C	ZIKV: LOD_{95}=22 PFU/mL; CHIKV: 10^3 PFU/mL; DENV-1: 10^3 copies/μL	[37]
	Hydrogel RT-LAMP	RT-LAMP+QUASR probe	NA	MRSA mecA, CREC blaNDM	2	65 °C	1 copy/reaction	[59]
Cleavage-dependent probes	MERT-LAMP	RT-LAMP+MERT	Nb.BsrDI	*Listeria monocytogenes* lmo0733, *Listeria ivanovii* smcL	2	64 °C	250 fg DNA/reaction	[60]
	TEC-LAMP	RT-LAMP+TEC	Tth endonuclease IV	*Streptococcus pneumoniae* SPNA45_01710, *Neisseria meningitidis* NMO_1242, *Haemophilus influenzae* pstA, IAC	4	67 °C	*S. pneumoniae*: 39.5 copies/reaction; *N. meningitidis*: 17.3 copies/reaction; *H. influenzae*: 25.9 copies/reaction (95% probit)	[61]
	Proofman	RT-LAMP+Proofman	Pfu polymerase	SARS-CoV-2 N, ORF1ab, IC	3	60 °C	100 copies/reaction	[62]
	HFman	RT-LAMP+HFman probe	Q5 polymerase	SARS-CoV-2 ORF, E, human β-actin (internal reference)	3	64 °C	115 copies/reaction	[63]
CRISPR	SHERLOCKv2	RPA+CRISPR Cas13/Cas12a cis/trans-cleavage	LwaCas13a, PsmCas13b, CcaCas13b, AsCas12a, EiCsm6/LsCsm6/TtCsm6	ZIKV ssRNA, DENV ssRNA, synthetic ssRNA, synthetic dsDNA	4	37 °C	2 aM	[27]
	CRISPRD	LAMP+CRISPR Cas13/Cas12 cis/trans-cleavage	HiT7 RNA polymerase, TccCas13a, HheCas13a, AapCas12b	HPV16 E6/E7, HPV18 E6/E7, human RNase P (internal reference)	3	56 °C	10 copies/μL	[36]
	RPA-CRISPR/Cas12,13	RPA+CRISPR Cas12a/Cas13a cis/trans-cleavage	LbaCas12a, LwaCas13a, T7 RNA polymerase	Norovirus GI (GI-NoV), Rotavirus A (A-RoV)	2	37 °C	10^2 copies/μL	[28]

SDR	COLUMBO	PCR/RPA+Cas9 R-loop+SDR	SpyCas9 (wild-type, H840A nickase, dCas9)	SARS-CoV-2 E, N1, N2; SARS-CoV-1; MERS-CoV; SARS-CoV-2 variants (Alpha S-gene H69/V70 deletion, Delta N-gene Q9 deletion)	3	37 °C	1 copy/μL	[56]
	CRISPR-TMSD	RPA/RT-RPA+Cas12a cis-cleavage+TMSD	LbaCas12a	EGFR mutations (L858R, T790M, delE746-A750); SARS-CoV-2 S mutations (N501Y, D614G)	3	37 °C (Cas12a); 25 °C (TMSD)	1 copy/μL	[66]
	TOA	PCR/RPA+Cas12a cis-cleavage	LbaCas12a	Clinically relevant mutations: EGFR (T790M, S768I), TP53 R248W, PARP1 T>G, BRAF V600E, PIK3CA E545D	NA	37 °C (Cas12); 0 °C	0.037%	[67]

Note: LOD, limit of detection; Ref., reference; RPA, recombinase polymerase amplification; RT-LAMP, reverse transcription loop-mediated isothermal amplification; MB, molecular beacon; DARQ, detection of amplification by release of quenching; QUASR, quenching of unincorporated amplification signal reporters; MERT-LAMP, multiple endonuclease restriction real-time loop-mediated isothermal amplification; TEC-LAMP, Tth endonuclease cleavage loop-mediated isothermal amplification; CRISPR, clustered regularly interspaced short palindromic repeats; Cas, CRISPR-associated; SDR, strand displacement reaction; TMSD, toehold-mediated strand displacement; TOA, toehold activator; PCR, polymerase chain reaction; DNA, deoxyribonucleic acid; RNA, ribonucleic acid; ssRNA, single-stranded RNA; dsDNA, double-stranded DNA; cfDNA, cell-free DNA; PFU, plaque-forming unit; MRSA, methicillin-resistant Staphylococcus aureus; SARS-CoV-2, severe acute respiratory syndrome coronavirus 2; ORF, open reading frame; WNV, West Nile virus; CHIKV, chikungunya virus; ZIKV, Zika virus; DENV, dengue virus; CREC, carbapenem-resistant Escherichia coli; IAC, internal amplification control; IC, internal control; SHERLOCKv2, specific high-sensitivity enzymatic reporter unlocking version 2; CRISPRD, CRISPR multiplexed diagnostic assay; HPV, human papillomavirus; RNase P, ribonuclease P; GI-NoV, genogroup I norovirus; A-RoV, group A rotavirus; COLUMBO, Cas9 R-loop usage for molecular beacon opening; EGFR, epidermal growth factor receptor; TP53, tumor protein p53; PARP1, poly(ADP-ribose) polymerase 1; BRAF, B-Raf proto-oncogene; PIK3CA, phosphatidylinositol-4,5-bisphosphate 3-kinase catalytic subunit alpha; NA, not applicable. Species names are italicized.

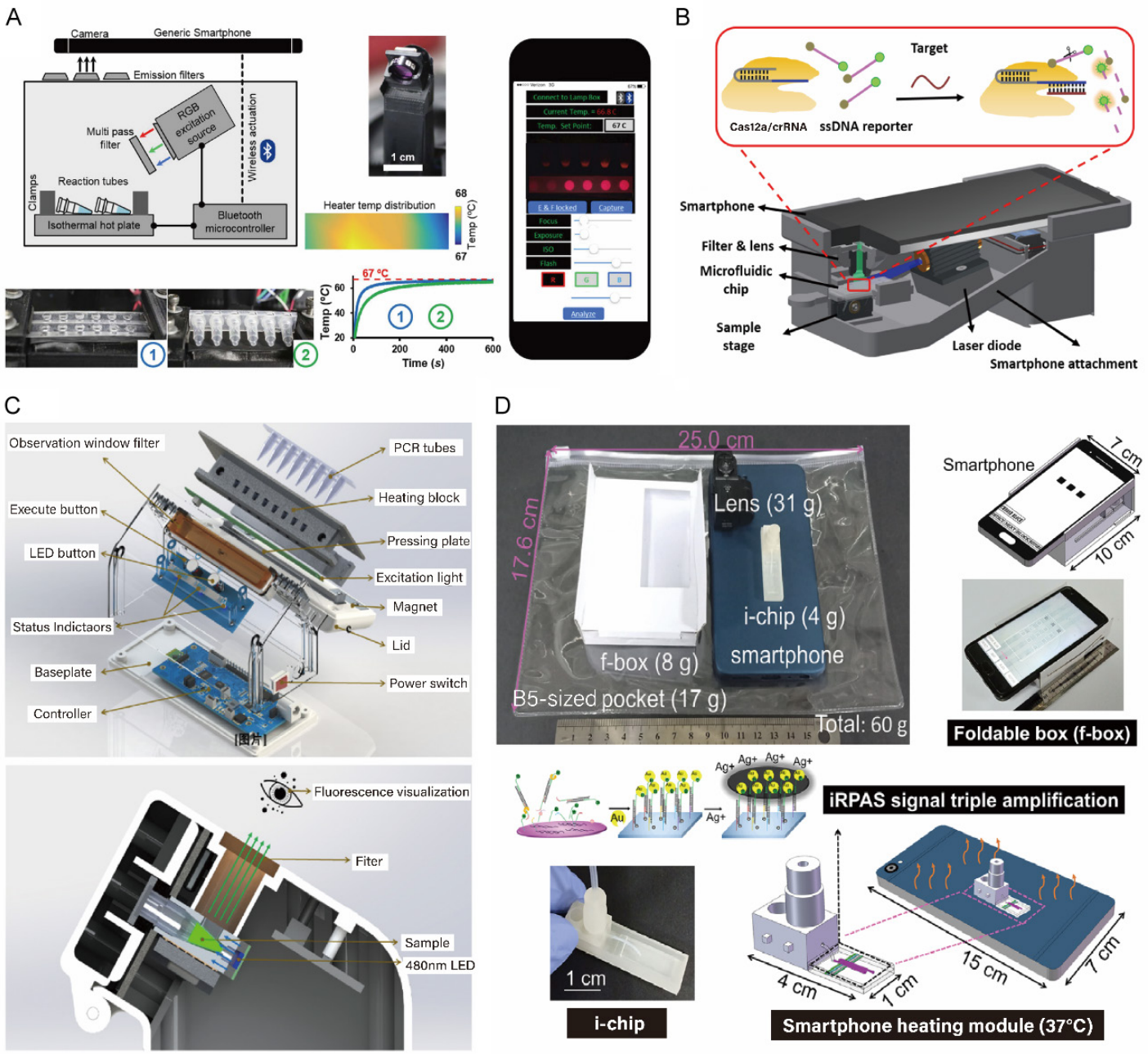

Figure 2. Schematic illustrations of portable fluorescence detection systems. (A) Structure of the LAMPbox portable detection platform; (B) Structure and detection principle of a 3D-printed portable smartphone attachment; (C) Internal structure of the WeD-1 handheld isothermal fluorescence detection device; (D) Structure and detection workflow of the fully integrated ultra-portable POCKET platform. This figure was cited from [25, 37, 46, 69]. temp, temperature; Cas12a, CRISPR-associated protein 12a; crRNA, CRISPR RNA; ssDNA, single-stranded DNA; PCR, polymerase chain reaction; LED, light-emitting diode; RGB, red-green-blue; iRPAS, integrated RNA purification and amplification system; i-chip, integrated chip; 3D, three-dimensional; POCKET, point-of-care kit for the entire test; E & F, exposure and focus; ISO, International Organization for Standardization.

cal utility was validated across 172 specimens, identifying both thalassemia mutations and urinary tract infection pathogens with area under the receiver operating characteristic (ROC) curve values ranging from 0.978 to 1.000, demonstrating 100% concordance with gold-standard methods.

4.2 Microfluidic chip integration: Automation and high throughput

The synergistic integration of high-throughput sample processing with portable optical detection has emerged as a significant

paradigm for achieving multiplex, high-sensitivity on-site testing.

Droplet microfluidics compartmentalizes the reaction mixture into tens of thousands of picoliter-scale droplets, enabling digital absolute quantification. The number of target molecules per droplet follows a Poisson distribution, allowing the initial concentration to be directly inferred by counting the number of positive droplets, thereby eliminating the need for a standard curve [70]. The CRISPR/Cas12a digital single-molecule microdroplet biosensor platform, developed by Zhao et al., integrates CRISPR/Cas12a detection with microdroplet technology to achieve amplification-free, duplex detection of meat adulteration [71]. The core innovation leverages the confinement effect of microdroplets, reducing the reaction volume to the picoliter scale and thereby increasing the local target concentration. This enhancement allows the collateral cleavage activity of Cas12a to detect targets at concentrations as low as 10 copies/μL, representing a 3×10^7-fold increase in sensitivity compared with conventional tube-based methods (**Figure 3A**). The droplet Cas12a detection platform developed by Yue et al. further harnessed this microfluidic strategy by dispersing Cas12a reaction volumes into millions of picoliter droplets [72]. By significantly enhancing reaction kinetics through localized concentration effects, this platform achieves absolute quantification of DNA at the single-molecule level without pre-amplification.

Chip-based microfluidics achieves multiplex detection through spatial encoding via physical partitioning, effectively circumventing spectral overlap limitations. The flap endonuclease 1-aided RPA-chip platform, developed by Ma et al., integrates flap endonuclease 1-assisted RPA with a self-priming microfluidic chip for high-plex pathogen screening [73]. The chip features a radial layout with 24 reaction chambers distributed around a central inlet, with fluidic connectivity established via microchannels. The chip is pre-degassed to generate negative pressure, facilitating autonomous sample loading without external pumps or valves (**Figure 3B**). Each chamber is preloaded with dried, target-specific probe mixtures, enabling position-encoded multiplex detection. In a 12-plex arbovirus detection assay, the platform achieved a sensitivity of 10 copies/reaction with excellent specificity and no cross-reactivity. When evaluated using 16 SARS-CoV-2-positive clinical samples, a 9-plex assay demonstrated 100% concordance with reverse transcription qPCR results. As illustrated in **Figure 3C**, the microfluidic device with CRISPR-Cas12a and multiplex RPA platform developed by Xu et al. combines the spatial encoding strategy with Cas12a detection [74]. By utilizing 48 independent reaction chambers on a microfluidic chip, the platform achieves parallel detection of nine HPV subtypes, demonstrating the potential of spatial encoding for clinical screening applications.

4.3 Intelligent diagnostic engineering: Intelligent signal analysis and generative design

As fluorescence isothermal amplification technologies advance toward higher throughput and greater multiplexing capacity, the dimensionality of the data generated by detection systems increases dramatically [64, 71]. Traditional manual interpretation and rudimentary threshold-based analysis are increasingly inadequate to meet the demands for accuracy, reproducibility, and efficiency. The introduction of intelligent signal analysis approaches—including automated image recognition and segmentation, feature extraction from fluorescence kinetic curves, and quantitative modeling through multi-parameter data fusion using machine learning algorithms—is fundamentally transforming the paradigm of fluorescence data processing [26, 71, 75]. These advances provide critical support for the on-site application and large-scale implementation of multiplex detection.

4.3.1 Image recognition and classification

In microfluidic and digital isothermal amplification, automated fluorescence image analysis is a prerequisite for accurate counting. Traditional image processing software (e.g., ImageJ) relies on manually defined thresholds, which are not only labor-intensive but also lack robustness against background noise and non-uniform illumination. The application of deep learning-based object detection models enables rapid and accurate identification and classification of multicolor fluorescent spots.

Yang et al. integrated QUASR with a hydrogel-based digital LAMP platform, leveraging the YOLOv8m algorithm to develop an AI-powered, color-encoded digital LAMP system [59]. The research team collected 4,773 manually annotated spot images to train the object detection model, which achieved rapid, automated identification and quantification of multicolor spots within 2–4 seconds, with higher accuracy than manual analysis using ImageJ. The system enabled single-copy-level multiplex quantification of bacteria across 10 different food matrices.

The versatile Multi-RPA-CRISPR/Cas12a-G4 portable chip developed by Li et al. utilizes the YOLOv5 object detection model to interpret colorimetric results from multi-chamber chips [75]. The researchers compiled a training set of 10,976 images and a validation set of 4,000 images, with the YOLOv5-s model achieving an mAP@0.5 of 0.996 and completing image analysis within 2–4 seconds. Following deployment as a smartphone app, users can simply upload a chip image to automatically obtain detection results. In genetically modified organism detection, the system achieved 93.3% accuracy with an LOD as low as 1 aM.

The R-CHIP platform, developed by Xu et al., integrates a hand-driven centrifugal microfluidic chip with the Residual

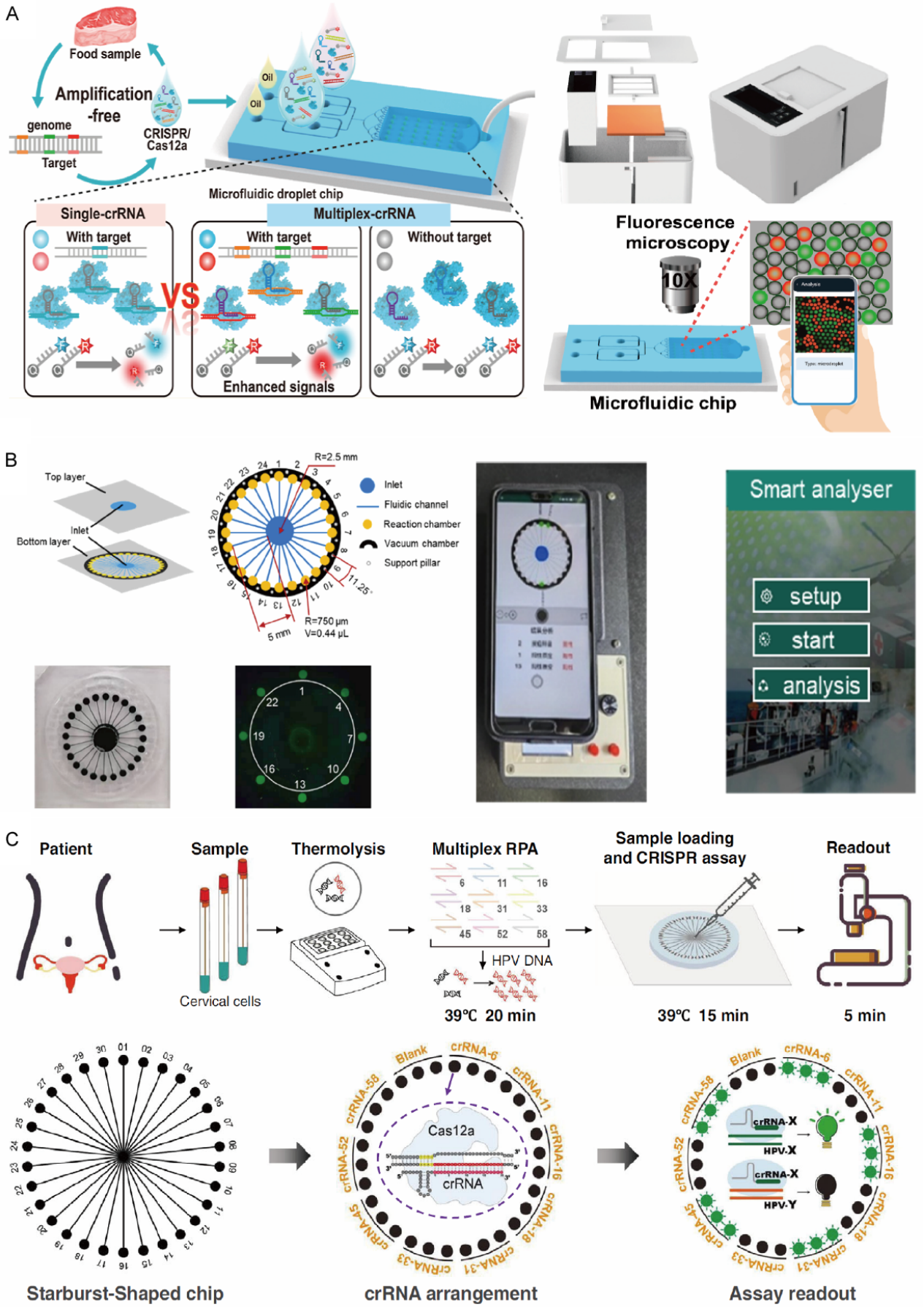
A
Food sample
Amplification -free
genome
Target
CRISPR/ Cas12a
Oil
Oil
Microfluidic droplet chip
Single-crRNA
With target
VS
Multiplex-crRNA
With target
Without target
Enhanced signals
Fluorescence microscopy
10X
Microfluidic chip
B
Top layer
Inlet
Bottom layer
R=2.5 mm
Inlet
Fluidic channel
Reaction chamber
Vacuum chamber
Support pillar
11.25°
5 mm
R=750 μm
V=0.44 μL
Smart analyser
setup
start
analysis
C
Patient
Sample
Thermolysis
Multiplex RPA
Sample loading and CRISPR assay
Readout
Cervical cells
HPV DNA
39℃ 20 min
39℃ 15 min
5 min
Starburst-Shaped chip
crRNA arrangement
Assay readout
Blank
crRNA-6
crRNA-11
crRNA-16
crRNA-18
crRNA-31
crRNA-33
crRNA-45
crRNA-52
crRNA-58
Cas12a
crRNA
crRNA-X
HPV-X
HPV-Y

Figure 3. Schematic illustration of integrated microfluidic systems. (A) Schematic illustration of the detection principle and workflow of the CC-drop platform; (B) Schematic illustration of the structure of the FARPA-chip platform; (C) Schematic illustration of the detection principle and workflow of the MiCaR platform. This figure was cited from [71, 73, 74]. CC-drop, CRISPR/Cas12a digital single-molecule microdroplet biosensor; FARPA, flap endonuclease 1-aided recombinase polymerase amplification; MiCaR, microfluidic device with CRISPR-Cas12a and multiplex recombinase polymerase amplification; CRISPR, clustered regularly interspaced short palindromic repeats; Cas12a, CRISPR-associated protein 12a; crRNA, CRISPR RNA; RPA, recombinase polymerase amplification; HPV, human papillomavirus.

Network-18 deep learning model for multiplex nucleic acid detection of high-risk HPV [76]. To optimize model performance, the researchers curated a dataset comprising 10,976 training and 4,000 validation images, utilizing data augmentation techniques to vary fluorescence intensities. Upon deploying the model on a smartphone, its performance was validated using 100 clinical cervical swab specimens. The model achieved an overall classification accuracy of 94.0%, with areas under the ROC curve exceeding 0.98 for all categories. The R-CHIP platform completes the entire workflow from sample lysis to automated readout within one hour, creating a closed loop between electricity-free, manual microfluidic operation and smartphone-based deep learning decoding. This offers an ideal solution for large-scale, intelligent high-risk HPV screening at the community level.

4.3.2 AI-assisted molecular tool development

Intelligent signal analysis transcends the post-detection data processing phase, progressively permeating the upstream development of detection systems through generative design and predictive modeling. AI models trained on large-scale datasets can uncover sequence-function relationships that are difficult to capture intuitively, significantly raising the performance ceiling of detection systems.

In predictive design, Wei et al. systematically elucidated the gRNA design principles for CRISPR-associated protein 13d effectors using convolutional neural networks (CNNs) [77]. This work established the most comprehensive gRNA functionality dataset to date, comprising 127,071 gRNAs targeting 55 essential genes and tens of thousands of control sequences. Robustness was evaluated on validation sets containing thousands of endogenous gene targets. When comparing the predictive performance of linear, ensemble, and deep learning models, CNNs exhibited the best performance (area under the ROC curve =0.845).

However, traditional predictive models often neglect the spatial conformational information of nucleic acid. Addressing this limitation, Riley et al. proposed a deep learning architecture named Sequence And Structure for RNA functional prediction [78]. This model innovatively incorporates the RNA secondary structure matrix as a matrix input channel parallel to sequence information. The key innovation of this model is its efficient 2D structural encoding—representing nucleotide base-pairing interactions as an N×N structural adjacency matrix—thereby enabling the CNN to autonomously learn structure-derived abstract features pertinent to molecular function. By processing the RNA secondary structure matrix in parallel with sequence information, the Sequence and Structure for RNA functional prediction model significantly outperformed sequence-only models and traditional thermodynamic methods in both simulated and real-world tasks. In complex systems such as aptaswitches, the model screened high-performance targeting sequences with a 10.7% improvement over Nucleic Acid Package designs using only 384 training samples.

To provide a systematic overview of this emerging interdisciplinary field, **Table 2** summarizes representative studies in intelligent signal analysis and AI-assisted molecular design, including the types of deep learning algorithms employed, dataset scales, and key performance metrics, thereby facilitating direct comparison of their capabilities and application scenarios.

The amalgamation of portable readouts, microfluidics, and deep learning signifies a profound paradigm shift in multiplex diagnostics: transitioning from hardware-reliant analytical chemistry to data-driven molecular informatics. By physically compartmentalizing reactions, microfluidics elegantly resolves the inherent spectral overlap bottleneck of fluorescence, while smartphone-based optics decentralize the diagnostic power. More importantly, the infusion of AI elevates the entire ecosystem from passive detection to proactive prediction. Moving forward, the ultimate diagnostic platforms will likely be highly miniaturized, fully automated, and seamlessly connected to cloud-based epidemiological networks, thereby transforming isolated POCT devices into distributed nodes for real-time global syndromic surveillance.

5 CONCLUSION

Despite significant strides in fluorescence isothermal amplification, translating laboratory prototypes into reliable POCT products remains challenging due to fundamental biochemical and physical bottlenecks. From a molecular perspective, the geometric increase in primer and probe complexity elevates the risk of cross-reactivity and false negatives, often necessitating extensive empirical optimization. In terms of signal encoding capacity, spectral overlap limits single-tube multiplexing to typically four targets, while spatial multiplexing via microfluidics introduces device complexity and higher sample consumption. Furthermore, amplification bias arises from compe-

Table 2. Summary of deep learning applications in intelligent signal analysis and molecular design for isothermal amplification

Application category	Deep learning model	Diagnostic platform/ target	Dataset	Key parameters/metrics	Ref.
Image recognition and classification	YOLOv8m	Hydrogel digital LAMP (MRSA, CRE)	4,773 spot images	Performance metrics: AUC=0.877; Ultrafast analysis time (2–4 s); Outperforms conventional manual thresholding (ImageJ). Validated across 10 diverse food matrices.	[59]
	Yolov5-s	Portable Multi-RPA-CRISPR/Cas12a-G4 chip (GMO: CaMV35S, NOS)	10,976 training images, 4,000 validation images	Performance metrics: mAP@0.5=0.996; Automated smartphone readout accuracy of 93.3%. Features: 1 aM LOD.	[75]
	ResNet-18	R-CHIP (HR-HPV 16/18)	10,976 training images, 4,000 validation images	Performance metrics: 94.0% overall accuracy for 4-class classification; macro- average AUC=0.9924. Validation: 100 clinical cervical swab samples. Features: 1 aM LOD.	[76]
Molecular design/prediction	CNN	Cas13d gRNA design (CasRx, DjCas13d)	Training: 127,071 CasRx gRNAs targeting 55 essential genes, 14,111 control gRNAs, and 3,563 non-targeting gRNAs (total 144,745); validation datasets include CD58/CD81 and CD46/CD55/CD71 in HEK293FT cells.	Performance metrics: AUROC=0.875; AUPRC=0.638. Validated across 5 endogenous genes with consistent AUROC>0.85. Features: High-confidence predictions (threshold ≥0.9) yielded up to 94% true positive rate.	[77]
	SANDSTORM+ GARDN	Functional RNA design (Toehold switches, 5' UTR, RBS, Cas13a gRNA, aptaswitch)	Functional RNA datasets: Toehold switches–Angenent-Mari et al.; 5' UTRs–Sample et al.; RBS–Höllerer et al.; CRISPR gRNAs–Metsky et al. (ADAPT dataset); Aptaswitch–custom 384-sequence small dataset	Performance metrics: Matches or outperforms SOTA models with 58%–95% fewer parameters; Ultrafast design speed (<1 s for whole-genome scan). Features: Exceptional few-shot learning capability (beats thermodynamic tools with minimal data); Maintains high 2D structural fidelity.	[78]

Note: AUC, Area Under the Curve; mAP@0.5, mean Average Precision at Intersection over Union (IoU) threshold of 0.5; AUPRC, Area Under the Precision–Recall Curve; AUROC, Area Under the Receiver Operating Characteristic Curve; MRSA, Methicillin-resistant Staphylococcus aureus; CRE, Carbapenem-resistant Enterobacteriaceae; LAMP, Loop-mediated Isothermal Amplification; RPA, Recombinase Polymerase Amplification; CRISPR, Clustered Regularly Interspaced Short Palindromic Repeats; Cas12a, CRISPR-associated protein 12a; Cas13a, CRISPR-associated protein 13a; Cas13d, CRISPR-associated protein 13d; GMO, Genetically Modified Organism; CaMV35S, Cauliflower Mosaic Virus 35S promoter; NOS, Nopaline Synthase terminator; HR-HPV, High-Risk Human Papillomavirus; RBS, Ribosome Binding Site; UTR, Untranslated Region; CNN, Convolutional Neural Network; SOTA, State-of-the-Art; LOD, Limit of Detection; aM, attomolar (10^{-18} M); HEK293FT, Human Embryonic Kidney 293FT cell line.

tition for shared resources, which disproportionately compromises the quantitative accuracy of highly homologous targets.

These intrinsic limitations are practically reflected in currently Food and Drug Administration-authorized LAMP products, which exhibit vast disparities in analytical sensitivity (up to a 200-fold difference for SARS-CoV-2) and often fall short of WHO clinical standards [19]. This highlights the persistent gap between technical feasibility and clinical reliability in complex infection scenarios.

Translating these methodologies into commercial-grade diagnostic platforms is further impeded by varying degrees of technical maturity and engineering hurdles. While spectral encoding strategies boast high technological readiness due to their compatibility with existing qPCR infrastructure, emerging approaches face formidable challenges. Orthogonal CRISPR-based detection struggles with multi-enzyme stability and batch-to-batch consistency, whereas SDR-based logic circuits remain largely at the proof-of-concept stage, hindered by the high synthesis costs of complex nucleic acid structures and their inherent instability in crude clinical samples.

Compounding these engineering challenges is the lack of standardized regulatory frameworks. The absence of unified performance evaluation metrics comparable to established qPCR

protocols complicates regulatory clearance. Furthermore, highly integrated microfluidic chips and multiplex drug-resistance panels demand rigorous companion diagnostic clinical trials. Additionally, as deep learning models increasingly augment CRISPR diagnostics, their 'black-box' nature necessitates the integration of explainable AI to navigate stringent regulatory pathways and facilitate clinical adoption.

Driven by the WHO's comprehensive REASSURED (real-time connected, easy to collect, affordable, sensitive, specific, user-friendly, rapid, robust, equipment-free, and deliverable) vision, the paradigm of diagnostic development is shifting from experience-driven to AI-driven design [79]. Deep learning and generative models now enable the prediction of gRNA sequences for 'day-zero' diagnostics of emerging variants, while protein language models guide the engineering of superior Cas enzymes. Consequently, multiplex isothermal amplification is transcending traditional infectious disease diagnosis, expanding into precision antimicrobial resistance panels, tumor liquid biopsies for early screening, and large-scale environmental and food safety monitoring.

Looking forward, the convergence of these advanced diagnostic technologies with wearable devices (e.g., bio-sensing face masks and pathogen-analyzing sweat patches) represents the next frontier of POCT [80, 81]. These innovations promise to redefine the diagnostic landscape by shifting from intermittent, symptom-triggered testing to continuous, non-invasive health monitoring. Ultimately, this transition will democratize access to accurate, intelligent diagnostic services, realizing a fundamental shift in global health governance and preemptive disease intervention.

DECLARATIONS

Author contributions

Xitian Xu and Yuanshou Zhu collected data, wrote the manuscript, revised the content, and performed proofreading. Yuanshou Zhu and Zhigang Zhu supervised the study and guided the writing and revision. Yuxin Chen, Mengyuan Huang, Shoulong Wang, and Haoyu Li provided technical support, contributed to literature review, and assisted in manuscript refinement.

Funding

This work was partially supported by the project "Research on the Development of a Detection Chip for Common Pathogens in Pet Dogs" (H-2024-312-025), and "Shanghai University Young Teacher Training Funding Program" (10-26-112-005-066), and University of Shanghai for Science and Technology Graduate Teaching Development Program (10-25-115-004-007).

Data availability

Not applicable.

Ethics approval and consent to participate

Not applicable.

Consent for publication

Not applicable.

Competing interests

The authors declare that they have no known competing financial interests or personal relationships that could have influenced the work reported in this paper.

Acknowledgements

We would like to thank the Biorender (Biorender.com) for drawing assistance.

REFERENCES

[1] Dorsey AF. Urbanization and infectious disease. Am J Hum Biol. 2025 Jan;37(1):e24197. https://doi.org/10.1002/ajhb.24197

[2] Ali A, Shaikh A, Sethi I, Surani S. Climate change and the emergence and exacerbation of infectious diseases: A review. World J Virol. 2024 Dec 25;13(4):96476. https://doi.org/10.5501/wjv.v13.i4.96476

[3] Bartlett ML, Miley K, Vermund SH, Weaver SC. Arthropod-borne disease challenges from planetary warming, urbanization, and migration. Virol J. 2025 Oct 10;22(1):325. https://doi.org/10.1186/s12985-025-02950-0

[4] Rudroff T. Climate crossroads: How global warming drives coronavirus emergence, the long COVID crisis of tomorrow, and AI's role in navigating our future. Infect Dis Now. 2025 Sep;55(6):105091. https://doi.org/10.1016/j.idnow.2025.105091

[5] Wang X, Li J, Liu H, Hu X, Lin Z, Xiong N. SARS-CoV-2 versus influenza A virus: Characteristics and co-treatments. Microorganisms. 2023 Feb 24;11(3):580. https://doi.org/10.3390/microorganisms11030580

[6] Teluguakula N, Chow VTK, Pandareesh MD, Dasegowda V, Kurrapotula V, Gopegowda SM, et al. SARS-CoV-2 and influenza co-infection: Fair competition or sinister combination? Viruses. 2024 May 16;16(5):793. https://doi.org/10.3390/v16050793

[7] Cerilo-Filho M, Arouca ML, Medeiros EDS, Jesus MC, Sampaio MP, Reis NF, et al. Worldwide distribution, symptoms and diagnosis of the coinfections between malaria and arboviral diseases: A systematic review. Mem Inst Oswaldo Cruz. 2024 Jun 24;119:e240015. https://doi.org/10.1590/0074-02760240015

[8] Yeoh YK, Zuo T, Lui G, Zhang F, Liu Q, Li A, et al. Gut microbiota composition reflects disease severity and dysfunctional immune responses in patients with COVID-19. Gut. 2021 Apr;70(4):698-706. https://doi.org/10.1136/gutjnl-2020-323020

[9] Zuo T, Zhang F, Lui G, Yeoh YK, Li A, Zhan H, et al. Alterations in gut microbiota of patients with COVID-19 during time of hospitalization. Gastroenterology. 2020 Sep;159(3):944-955.e8. https://doi.org/10.1053/j.gastro.2020.05.048

[10] Niemz A, Ferguson TM, Boyle DS. Point-of-care nucleic acid testing for infectious diseases. Trends Biotechnol. 2011 May; 29(5):240-250. https://doi.org/10.1016/j.tibtech.2011.01.007

[11] Yang S, Rothman RE. PCR-based diagnostics for infectious diseases: Uses, limitations, and future applications in acute-care settings. Lancet Infect Dis. 2004 Jun;4(6):337-348. https://doi.org/10.1016/S1473-3099(04)01044-8

[12] Mabey D, Peeling RW, Ustianowski A, Perkins MD. Diagnostics for the developing world. Nat Rev Microbiol. 2004 Mar;2(3):231-240. https://doi.org/10.1038/nrmicro841

[13] Yu Y, Zhou J, Li B, Ji M, Wang Y, Carnaby E, et al. A quantitative RT-qLAMP for the detection of SARS-CoV-2 and human gene in clinical application. Microb Biotechnol. 2022 Oct; 15(10):2619-2630. https://doi.org/10.1111/1751-7915.14112

[14] Daher RK, Stewart G, Boissinot M, Bergeron MG. Recombinase polymerase amplification for diagnostic applications. Clin Chem. 2016 Jul;62(7):947-958. https://doi.org/10.1373/clinchem.2015.245829

[15] Becherer L, Borst N, Bakheit M, Frischmann S, Zengerle R, von Stetten F. Loop-mediated isothermal amplification (LAMP)–review and classification of methods for sequence-specific detection. Anal Methods. 2020;12(6):717-746. https://doi.org/10.1039/C9AY02246E

[16] Tomita N, Mori Y, Kanda H, Notomi T. Loop-mediated isothermal amplification (LAMP) of gene sequences and simple visual detection of products. Nat Protoc. 2008;3(5):877-882. https://doi.org/10.1038/nprot.2008.57

[17] Tanner NA, Zhang Y, Evans TC Jr. Visual detection of isothermal nucleic acid amplification using pH-sensitive dyes. Biotechniques. 2015 Feb 1;58(2):59-68. https://doi.org/10.2144/000114253

[18] Tanner NA, Zhang Y, Evans TC Jr. Simultaneous multiple target detection in real-time loop-mediated isothermal amplification. Biotechniques. 2012 Aug;53(2):81-89. https://doi.org/10.2144/0000113902

[19] Jin A, Deng M, Yang H, Li Z. Loop-mediated isothermal amplification (LAMP)-based microbial detection: A review of FDA-authorized tests and future perspectives. Crit Rev Clin Lab Sci. 2026 Jan;63(1):57-79. https://doi.org/10.1080/10408363.2025.2542808

[20] Zhao Y, Chen F, Li Q, Wang L, Fan C. Isothermal amplification of nucleic acids. Chem Rev. 2015 Nov 25;115(22):12491-12545. https://doi.org/10.1021/acs.chemrev.5b00428

[21] Holland PM, Abramson RD, Watson R, Gelfand DH. Detection of specific polymerase chain reaction product by utilizing the 5'-3'exonuclease activity of Thermus aquaticus DNA polymerase. Proc Natl Acad Sci U S A. 1991 Aug 15;88(16):7276-7280. https://doi.org/10.1073/pnas.88.16.7276

[22] Gootenberg JS, Abudayyeh OO, Lee JW, Essletzbichler P, Dy AJ, Joung J, et al. Nucleic acid detection with CRISPR-Cas13a/C2c2. Science. 2017 Apr 28;356(6336):438-442. https://doi.org/10.1126/science.aam9321

[23] Chen JS, Ma E, Harrington LB, Da Costa M, Tian X, Palefsky JM, et al. CRISPR-Cas12a target binding unleashes indiscriminate single-stranded DNase activity. Science. 2018 Apr 27;360(6387):436-439. https://doi.org/10.1126/science.aar6245

[24] Li Y, Zhao L, Kang W, Ma L, Bai Y, Feng F. Multiplexed CRISPR/Cas and argonaute detection technology: Strategies, challenges, and perspectives. Trends Analyt Chem. 2025; 191:118329. https://doi.org/10.1016/j.trac.2025.118329

[25] Yu T, Zhang S, Matei R, Marx W, Beisel CL, Wei Q. Coupling smartphone and CRISPR–Cas12a for digital and multiplexed nucleic acid detection. AIChE J. 2021;67(12):e173652021. https://doi.org/10.1002/aic.17365

[26] Li Q, Lin X. AI-enhanced CRISPR diagnostics: From gRNA design to Cas protein engineering and signal analytics. Trends Analyt Chem. 2026;197:118704. https://doi.org/10.1016/j.trac.2026.118704

[27] Gootenberg JS, Abudayyeh OO, Kellner MJ, Joung J, Collins JJ, Zhang F. Multiplexed and portable nucleic acid detection platform with Cas13, Cas12a, and Csm6. Science. 2018 Apr 27;360(6387):439-444. https://doi.org/10.1126/science.aaq0179

[28] Le X, Jiang J, Hong Y, Shi J, Liu X, Xue J, et al. Development of an on-site real-time dual detection method for norovirus and rotavirus using RPA-CRISPR/Cas12,13. Food Control. 2025; 168:110943. https://doi.org/10.1016/j.foodcont.2024.110943

[29] Notomi T, Okayama H, Masubuchi H, Yonekawa T, Watanabe K, Amino N, et al. Loop-mediated isothermal amplification of DNA. Nucleic Acids Res. 2000;28(12):e63. https://doi.org/10.1093/nar/28.12.e63

[30] Thompson TZ, McMullen AR. Group A streptococcus testing in pediatrics: The move to point-of-care molecular testing. J Clin Microbiol. 2020 May 26;58(6):e01494-19. https://doi.org/10.1128/jcm.01494-19

[31] Rohatensky MG, Livingstone DM, Mintchev P, Barnes HK, Nakoneshny SC, Demetrick DJ, et al. Assessing the performance of a loop mediated isothermal amplification (LAMP) assay for the detection and subtyping of high-risk suptypes of human papilloma virus (HPV) for oropharyngeal squamous cell carcinoma (OPSCC) without DNA purification. BMC Cancer. 2018 Feb 8;18(1):166. https://doi.org/10.1186/s12885-018-4087-1

[32] Walker FM, Hsieh K. Advances in directly amplifying nucleic acids from complex samples. Biosensors (Basel). 2019 Sep 30;9(4):117. https://doi.org/10.3390/bios9040117

[33] Rolando JC, Jue E, Barlow JT, Ismagilov RF. Real-time kinetics and high-resolution melt curves in single-molecule digital LAMP to differentiate and study specific and non-specific amplification. Nucleic Acids Res. 2020 Apr 17;48(7):e42. https://doi.org/10.1093/nar/gkaa099

[34] Piepenburg O, Williams CH, Stemple DL, Armes NA. DNA detection using recombination proteins. PLoS Biol. 2006 Jul;4(7):e204. https://doi.org/10.1371/journal.pbio.0040204

[35] Lobato IM, O'Sullivan CK. Recombinase polymerase amplification: Basics, applications and recent advances. Trends Analyt

Chem. 2018 Jan;98:19-35. https://doi.org/10.1016/j.trac.2017.10.015

[36] Ghouneimy A, Ali Z, Aman R, Jiang W, Aouida M, Mahfouz M. CRISPR-based multiplex detection of human papillomaviruses for one-pot point-of-care diagnostics. ACS Synth Biol. 2024 Mar 15;13(3):837-850. https://doi.org/10.1021/acssynbio.3c00655

[37] Priye A, Bird SW, Light YK, Ball CS, Negrete OA, Meagher RJ. A smartphone-based diagnostic platform for rapid detection of Zika, chikungunya, and dengue viruses. Sci Rep. 2017 Mar 20;7:44778. https://doi.org/10.1038/srep44778

[38] Lutz S, Weber P, Focke M, Faltin B, Hoffmann J, Müller C, et al. Microfluidic lab-on-a-foil for nucleic acid analysis based on isothermal recombinase polymerase amplification (RPA). Lab Chip. 2010 Apr 7;10(7):887-893. https://doi.org/10.1039/B921140C

[39] Brouns SJ, Jore MM, Lundgren M, Westra ER, Slijkhuis RJ, Snijders AP, et al. Small CRISPR RNAs guide antiviral defense in prokaryotes. Science. 2008 Aug 15;321(5891):960-964. https://doi.org/10.1126/science.1159689

[40] Mohanraju P, Makarova KS, Zetsche B, Zhang F, Koonin EV, Van der Oost J. Diverse evolutionary roots and mechanistic variations of the CRISPR-Cas systems. Science. 2016 Aug 5;353(6299):aad5147. https://doi.org/10.1126/science.aad5147

[41] Makarova KS, Wolf YI, Iranzo J, Shmakov SA, Alkhnbashi OS, Brouns SJ, et al. Evolutionary classification of CRISPR–Cas systems: A burst of class 2 and derived variants. Nat Rev Microbiol. 2020 Feb;18(2):67-83. https://doi.org/10.1038/s41579-019-0299-x

[42] Jinek M, Chylinski K, Fonfara I, Hauer M, Doudna JA, Charpentier E. A programmable dual-RNA–guided DNA endonuclease in adaptive bacterial immunity. Science. 2012 Aug 17;337(6096):816-821. https://doi.org/10.1126/science.1225829

[43] Teng F, Guo L, Cui T, Wang X, Xu K, Gao Q, et al. CDetection: CRISPR-Cas12b-based DNA detection with sub-attomolar sensitivity and single-base specificity. Genome Biol. 2019 Jul 1;20(1):132. https://doi.org/10.1186/s13059-019-1742-z

[44] Abudayyeh OO, Gootenberg JS, Konermann S, Joung J, Slaymaker IM, Cox DB, et al. C2c2 is a single-component programmable RNA-guided RNA-targeting crispr effector. Science. 2016 Aug 5;353(6299):aaf5573. https://doi.org/10.1126/science.aaf5573

[45] Li S, Cheng Q, Liu J, Nie X, Zhao G, Wang J. CRISPR-Cas12a has both cis-and trans-cleavage activities on single-stranded DNA. Cell Res. 2018 Apr;28(4):491-493. https://doi.org/10.1038/s41422-018-0022-x

[46] Pang F, Zhang T, Dai F, Wang K, Jiao T, Zhang Z, et al. A handheld isothermal fluorescence detector for duplex visualization of aquatic pathogens via enhanced one-pot LAMP-PfAgo assay. Biosens Bioelectron. 2024 Jun 15;254:116187. https://doi.org/10.1016/j.bios.2024.116187

[47] Yurke B, Turberfield AJ, Mills AP Jr, Simmel FC, Neumann JL. A DNA-fuelled molecular machine made of DNA. Nature. 2000 Aug 10;406(6796):605-608. https://doi.org/10.1038/35020524

[48] Srinivas N, Ouldridge TE, Šulc P, Schaeffer JM, Yurke B, Louis AA, et al. On the biophysics and kinetics of toehold-mediated DNA strand displacement. Nucleic Acids Res. 2013 Dec;41(22):10641-10658. https://doi.org/10.1093/nar/gkt801

[49] Park JW. Principles and applications of loop-mediated isothermal amplification to point-of-care tests. Biosensors (Basel). 2022 Oct 10;12(10):857. https://doi.org/10.3390/bios12100857

[50] Zhang D, Winfree E. Control of DNA strand displacement kinetics using toehold exchange. J Am Chem Soc. 2009 Dec 2;131(47):17303-17314. https://doi.org/10.1021/ja906987s

[51] Dirks RM, Pierce NA. Triggered amplification by hybridization chain reaction. Proc Natl Acad Sci U S A. 2004 Oct 26;101(43):15275-15278. https://doi.org/10.1073/pnas.0407024101

[52] Ma L, Liao D, Zhao Z, Kou J, Guo H, Xiong X, et al. Sensitive small molecule aptasensing based on hybridization chain reaction and CRISPR/Cas12a using a portable 3D-printed visualizer. ACS Sens. 2023 Mar 24;8(3):1076-1084. https://doi.org/10.1021/acssensors.2c02097

[53] Bai T, Qu X, Pan J, Tang Y, Wang L, Zhou P, et al. CRISPR-initiated exponential amplification on fluorescently-barcoded microspheres for deep learning-assisted multiplexed HPV detection. Biosens Bioelectron. 2026 May 15;300:118488. https://doi.org/10.1016/j.bios.2026.118488

[54] Zadeh JN, Steenberg CD, Bois JS, Wolfe BR, Pierce MB, Khan AR, et al. NUPACK: Analysis and design of nucleic acid systems. J Comput Chem. 2011 Jan 15;32(1):170-173. https://doi.org/10.1002/jcc.21596

[55] Poppleton E, Romero R, Mallya A, Rovigatti L, Šulc P. OxDNA.org: A public webserver for coarse-grained simulations of DNA and RNA nanostructures. Nucleic Acids Res. 2021 Jul 2;49(W1):W491-W498. https://doi.org/10.1093/nar/gkab324

[56] Marquez-Costa R, Montagud-Martinez R, Marques MC, Albert E, Navarro D, Daros JA, et al. Multiplexable and biocomputational virus detection by CRISPR-Cas9-mediated strand displacement. Anal Chem. 2023 Jun 27;95(25):9564-9574. https://doi.org/10.1021/acs.analchem.3c01041

[57] Ball CS, Light YK, Koh CY, Wheeler SS, Coffey LL, Meagher RJ. Quenching of unincorporated amplification signal reporters in reverse-transcription loop-mediated isothermal amplification enabling bright, single-step, closed-tube, and multiplexed detection of RNA viruses. Anal Chem. 2016 Apr 5;88(7):3562-3568. https://doi.org/10.1021/acs.analchem.5b04054

[58] Talap J, Shen M, Yu L, Zeng S, Cai S. RT-LAMP assay combining multi-fluorescent probes for SARS-CoV-2 RNA detection and variant differentiation. Talanta. 2022 Oct 1;248:123644. https://doi.org/10.1016/j.talanta.2022.123644

[59] Yang T, Zhang X, Yan Y, Liu Y, Lin X, Li W. Artificial intelligence-driven quantification of antibiotic-resistant Bacteria in food by color-encoded multiplex hydrogel digital LAMP. Food Chem. 2025 Mar 15;468:142304. https://doi.org/10.1016/j.foodchem.2024.142304

[60] Wang Y, Wang Y, Lan R, Xu H, Ma A, Li D, et al. Multiple endonuclease restriction real-time loop-mediated isothermal amplification: A novel analytically rapid, sensitive, multiplex loop-mediated isothermal amplification detection technique. J

Mol Diagn. 2015 Jul;17(4):392-401. https://doi.org/10.1016/j.jmoldx.2015.03.002

[61] Higgins O, Clancy E, Cormican M, Boo TW, Cunney R, Smith TJ. Evaluation of an internally controlled multiplex Tth endonuclease cleavage loop-mediated isothermal amplification (TEC-LAMP) assay for the detection of bacterial meningitis pathogens. Int J Mol Sci. 2018 Feb 9;19(2):524. https://doi.org/10.3390/ijms19020524

[62] Ding S, Chen G, Wei Y, Dong J, Du F, Cui X, et al. Sequence-specific and multiplex detection of COVID-19 virus (SARS-CoV-2) using proofreading enzyme-mediated probe cleavage coupled with isothermal amplification. Biosens Bioelectron. 2021 Apr 15;178:113041. https://doi.org/10.1016/j.bios.2021.113041

[63] Dong Y, Zhao Y, Li S, Wan Z, Lu R, Yang X, et al. Multiplex, real-time, point-of-care RT-LAMP for SARS-CoV-2 detection using the HFman probe. ACS Sens. 2022 Mar 25;7(3):730-739. https://doi.org/10.1021/acssensors.1c02079

[64] Ackerman CM, Myhrvold C, Thakku SG, Freije CA, Metsky HC, Yang DK, et al. Massively multiplexed nucleic acid detection with Cas13. Nature. 2020 Jun;582(7811):277-282. https://doi.org/10.1038/s41586-020-2279-8

[65] Tian T, Qiu Z, Jiang Y, Zhu D, Zhou X. Exploiting the orthogonal CRISPR-Cas12a/Cas13a trans-cleavage for dual-gene virus detection using a handheld device. Biosens Bioelectron. 2022 Jan 15;196:113701. https://doi.org/10.1016/j.bios.2021.113701

[66] Fu J, Zhang L, Long Y, Liu Z, Meng G, Zhao H, et al. Multiplexed CRISPR-based nucleic acid detection using a single Cas protein. Anal Chem. 2023 Nov 7;95(44):16089-16097. https://doi.org/10.1021/acs.analchem.3c01861

[67] Zhang W, Mu Y, Dong K, Zhang L, Yan B, Hu H, et al. PAM-independent ultra-specific activation of CRISPR-Cas12a via sticky-end dsDNA. Nucleic Acids Res. 2022 Dec 9;50(22):12674-12688. https://doi.org/10.1093/nar/gkac1144

[68] Marpaung DSS, Sinaga AOY. Toehold-mediated strand displacement in CRISPR/Cas12a reactions: Advances in programmable and universal biosensing strategies. Talanta. 2026 May 15;302:129442. https://doi.org/10.1016/j.talanta.2026.129442

[69] Xu H, Xia A, Wang D, Zhang Y, Deng S, Lu W, et al. An ultra-portable and versatile point-of-care DNA testing platform. Sci Adv. 2020 Apr 22;6(17):eaaz7445. https://doi.org/10.1126/sciadv.aaz7445

[70] Hindson BJ, Ness KD, Masquelier DA, Belgrader P, Heredia NJ, Makarewicz AJ, et al. High-throughput droplet digital PCR system for absolute quantitation of DNA copy number. Anal Chem. 2011 Nov 15;83(22):8604-8610. https://doi.org/10.1021/ac202028g

[71] Zhao Z, Wang R, Yang X, Jia J, Zhang Q, Ye S, et al. Machine learning-assisted, dual-channel CRISPR/Cas12a biosensor-in-microdroplet for amplification-free nucleic acid detection for food authenticity testing. ACS Nano. 2024 Dec 10;18(49):33505-33519. https://doi.org/10.1021/acsnano.4c10823

[72] Yue H, Shu B, Tian T, Xiong E, Huang M, Zhu D, et al. Droplet Cas12a assay enables DNA quantification from unamplified samples at the single-molecule level. Nano Lett. 2021 Jun 9;21(11):4643-4653. https://doi.org/10.1021/acs.nanolett.1c00715

[73] Ma Y, Wang Y, Chen C, Feng L, Shan J, Zhang L, et al. FEN1-Aided RPA (FARPA) coupled with autosampling microfluidic chip enables highly multiplexed on-site pathogen screening. Anal Chem. 2025 Mar 18;97(10):5762-5770. https://doi.org/10.1021/acs.analchem.4c07015

[74] Xu Z, Chen D, Li T, Yan J, Zhu J, He T, et al. Microfluidic space coding for multiplexed nucleic acid detection via CRISPR-Cas12a and recombinase polymerase amplification. Nat Commun. 2022 Oct 29;13(1):6480. https://doi.org/10.1038/s41467-022-34086-y

[75] Li X, Liu M, Xia X, Zeng X, Men D, Duan Y, et al. Deep learning assisted, smartphone based universal multi-RPA-CRISPR/Cas12a-G4 portable chip for simultaneous detection of CaMV35S and NOS. Food Control. 2025;168:110947. https://doi.org/10.1016/j.foodcont.2024.110947

[76] Xu T, Zhang Y, Li S, Dai C, Wei H, Chen D, et al. Deep learning-enhanced hand-driven microfluidic chip for multiplexed nucleic acid detection based on RPA/CRISPR. Adv Sci (Weinh). 2025 Jun;12(21):e2414918. https://doi.org/10.1002/advs.202414918

[77] Wei J, Lotfy P, Faizi K, Baungaard S, Gibson E, Wang E, et al. Deep learning and CRISPR-Cas13d ortholog discovery for optimized RNA targeting. Cell Syst. 2023 Dec;14(12):1087-1102.e13. https://doi.org/10.1016/j.cels.2023.11.006

[78] Riley AT, Robson JM, Ulanova A, Green AA. Generative and predictive neural networks for the design of functional RNA molecules. Nat Commun. 2025 May 4;16(1):4155. https://doi.org/10.1038/s41467-025-59389-8

[79] Land KJ, Boeras DI, Chen X, Ramsay AR, Peeling RW. REASSURED diagnostics to inform disease control strategies, strengthen health systems and improve patient outcomes. Nat Microbiol. 2019 Jan;4(1):46-54. https://doi.org/10.1038/s41564-018-0295-3

[80] Nguyen PQ, Soenksen LR, Donghia NM, Angenent-Mari NM, de Puig H, Huang A, et al. Wearable materials with embedded synthetic biology sensors for biomolecule detection. Nat Biotechnol. 2021 Nov;39(11):1366-1374. https://doi.org/10.1038/s41587-021-00950-3

[81] Sempionatto JR, Jeerapan I, Krishnan S, Wang J. Wearable chemical sensors: Emerging systems for on-body analytical chemistry. Anal Chem. 2020 Jan 7;92(1):378-396. https://doi.org/10.1021/acs.analchem.9b04668